

A *Ka*-Band 64-Element Deployable Active Phased-Array TX on a Flexible Hetero Segmented Liquid Crystal Polymer for Small Satellites

Dongwon You^{ID}, *Graduate Student Member, IEEE*, Xi Fu, *Member, IEEE*,
Hans Herdian^{ID}, *Graduate Student Member, IEEE*, Xiaolin Wang, *Student Member, IEEE*,
Yasuto Narukiyo, Ashbir Aviat Fadila^{ID}, *Graduate Student Member, IEEE*, Hojun Lee,
Michihiro Ide^{ID}, *Graduate Student Member, IEEE*, Sena Kato, *Student Member, IEEE*,
Zheng Li^{ID}, *Graduate Student Member, IEEE*, Yun Wang^{ID}, *Member, IEEE*, Daisuke Awaji,
Jian Pang^{ID}, *Member, IEEE*, Hiraku Sakamoto, Kenichi Okada^{ID}, *Fellow, IEEE*,
and Atsushi Shirane, *Member, IEEE*

Abstract—A *Ka*-band 64-element deployable active phased-array transmitter (TX) on a hetero segment liquid crystal polymer (LCP) substrate for small satellites is proposed. The proposed phased-array TX achieved a large array size implementation and a small form factor with integrated six-layer and two-layer LCP substrates. Antenna and transmission line designs considering hetero layer structure are presented in detail. Achieving 46.7 dBm electronically isotropically radiated power (EIRP), the proposed phased-array TX can support 256-APSK DVB-S2X. As a result, the proposed deployable active phased-array TX successfully realizes low-launch cost with a 9.65 g lightweight and large antenna aperture size with superior EVM performance.

Index Terms—Deployable, flexible, liquid crystal polymer (LCP), phased array, SATCOM, transmitter (TX).

I. INTRODUCTION

AS THE low earth orbit (LEO) small-satellites have been proven as a key solution in the low-cost and low-latency

Manuscript received 27 February 2023; accepted 1 April 2023. This work was supported in part by the Ministry of Internal Affairs and Communications (MIC)/Strategic Information and Communications Research and Development Promotion Programme (SCOPE) under Grant 192203002 and Grant 192103003; in part by the Japan Society for the Promotion of Science (JSPS) under Grant JP20H00236; in part by the MIC under Grant JPJ000254; in part by the Japan Science and Technology Agency (JST)/Adaptable and Seamless Technology transfer Program through target-driven Research and Development (A-STEP) under Grant JPMJTR211D; in part by the National Institute of Information and Communications Technology (NICT) under Grant 060601; in part by the Support for Tokyo Tech Advanced Researchers (STAR); and in part by the VLSI Design and Education Center (VDEC) in collaboration with Cadence Design Systems, Inc., Mentor Graphics, Inc., and Keysight Technologies Japan, Ltd. (*Corresponding author: Dongwon You.*)

Dongwon You, Xi Fu, Hans Herdian, Xiaolin Wang, Yasuto Narukiyo, Ashbir Aviat Fadila, Hojun Lee, Michihiro Ide, Sena Kato, Zheng Li, Yun Wang, Jian Pang, Kenichi Okada, and Atsushi Shirane are with the Department of Electrical and Electronic Engineering, Tokyo Institute of Technology, Tokyo 152-8552, Japan (e-mail: dongwon.wave@gmail.com).

Daisuke Awaji is with the Wideband Radio System Development, Electronic Technologies RDcenter, Fujikura Ltd., Tokyo 135-0042, Japan.

Hiraku Sakamoto is with the Department of Mechanical Engineering, Tokyo Institute of Technology, Tokyo 152-8552, Japan.

This article was presented at the IEEE MTT-S International Microwave Symposium (IMS 2023), San Diego, CA, USA, June 11–16, 2023.

Color versions of one or more figures in this letter are available at <https://doi.org/10.1109/LMWT.2023.3264810>.

Digital Object Identifier 10.1109/LMWT.2023.3264810

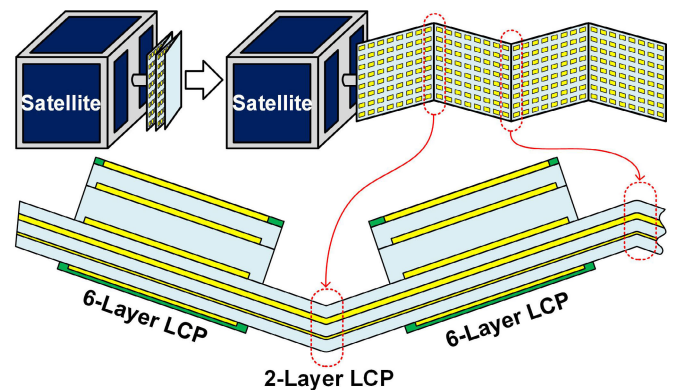


Fig. 1. Deployable active phased array with flex hetero segment LCP board.

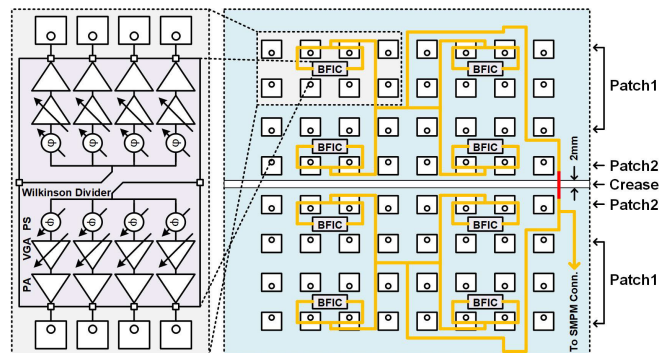


Fig. 2. Architecture of the proposed deployable active phased-array TX.

new-space era, their low form factor and large antenna aperture requirements are being further emphasized. The high output power from a power amplifier (PA) and high antenna gain are obviously critical to construct the long-distance link to the ground station from the satellite. However, the big size and heavy weight of the antenna result in an increase in the satellite launch cost. The deployable phased array is one of the most prominent solutions in the SATCOM applications for a smaller size yet with a large aperture area as shown in Fig. 1.

As revealing the importance of breaking through the trade-off between low form factor and large antenna aperture in SATCOM, a lot of deployable phased arrays have been reported [1], [2], [3], [4], [5], [6], [7]. In [1], two separate

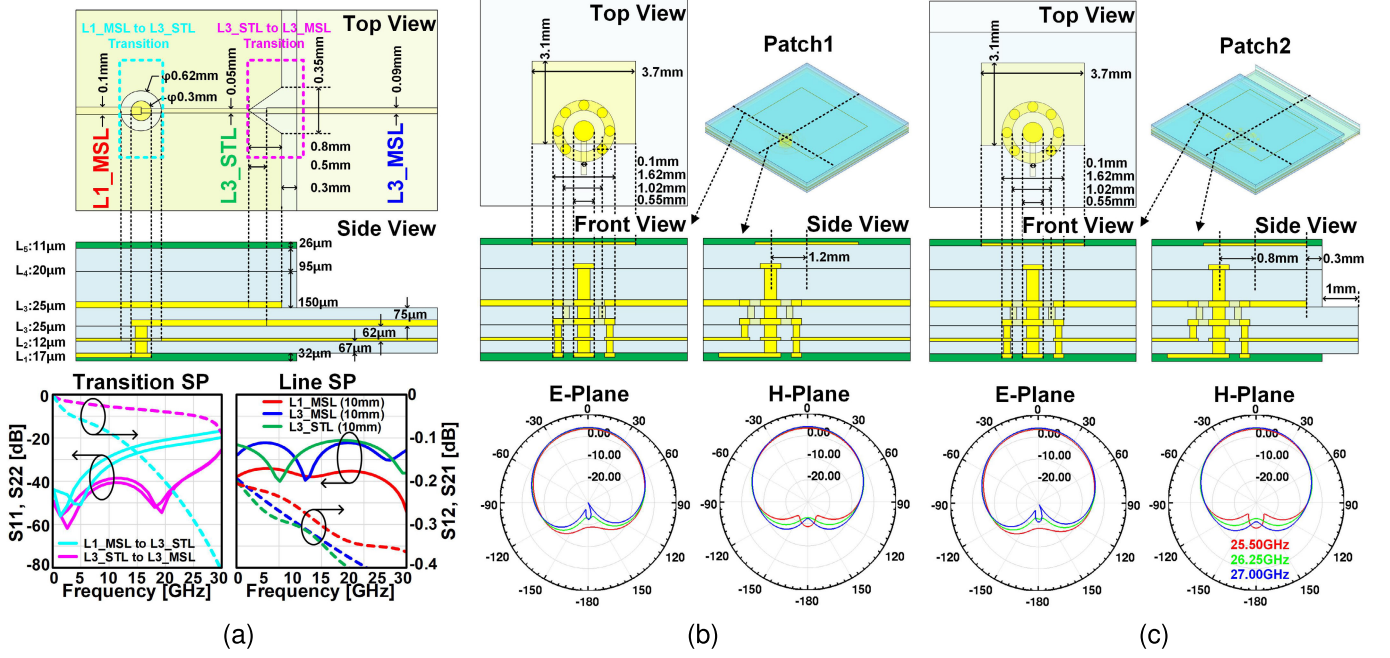


Fig. 3. 3-D models and simulation results of (a) three types of transmission lines, (b) patch antenna far from the crease, and (c) patch antenna near the crease.

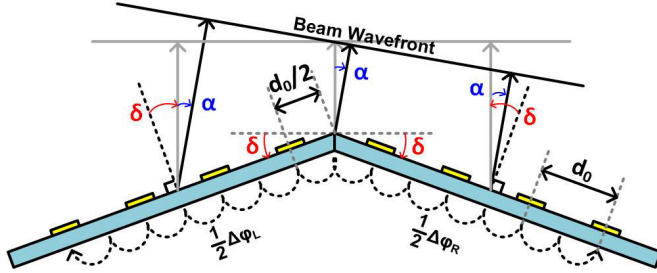


Fig. 4. Diagram for beam forming calibration against the bent board.

Megtron6 rigid substrates are connected with co-axial cables with SMPS connectors to realize deployability for the phased array design. However, rigid substrates are thick and heavy. Also, in large array construction, connecting all sub-arrays by coaxial cables is challenging. For lightweight and large array implementation, the fully flexible substrate is the efficient solution [2], [3], [4], [5], [6], [7]. The phased arrays in [2], [3], [4], and [5] adopted the polyimide for the deployable phased array. Meanwhile, polyimide substrates have an inferior dielectric loss and difficulties in multi-layer fabrication than liquid crystal polymer (LCP) substrates [6], [7]. Although one LCP substrate phased array has been reported in [6], because of a small number of layers, large array implementation is still challenging.

In this work, a Ka -band 64-element deployable active phased array transmitter (TX) on a flex hetero segment LCP board, integrating two-layer and six-layer LCP substrates, is presented to achieve a large array size and better flexibility.

II. DEPLOYABLE ACTIVE PHASED ARRAY DESIGN

A. Phased Array Architecture

Fig. 2 illustrates a block diagram of the proposed deployable active phased-array TX on the flex hetero segment LCP board. In this design, beamformer ICs (BFIC) in [8] are utilized onto a six-layer LCP active phased array board. The BFIC

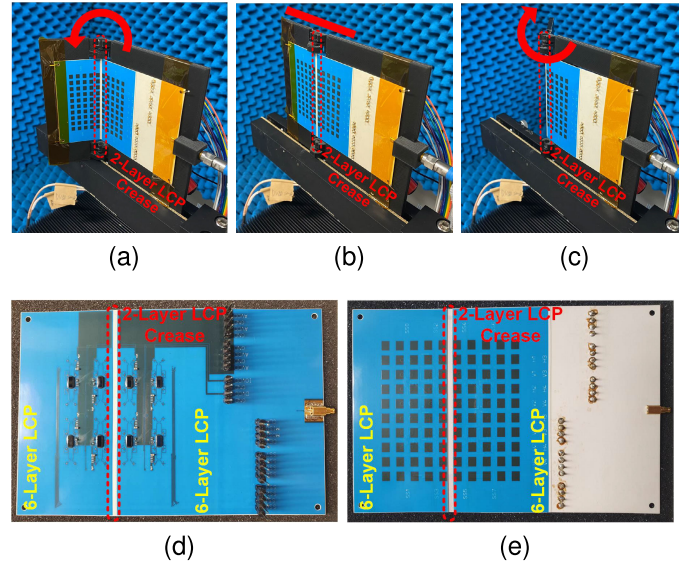


Fig. 5. Photographs of the fabricated deployable phased array: (a) with negative bent-angle; (b) with flat state; (c) with positive bent-angle; (d) of BFIC side; and (e) of antenna side.

is composed of eight paths of PA, phase shifter (PS), and variable gain amplifier chains. Eight BFICs are soldered and drive 64 patch antennas through microstrip lines on the first layer, L_1 , ($L1_MSL$). Each BFIC is driven by microstrip lines on the third layer, L_3 , ($L3_MSL$) and strip lines on the third layer, L_3 , ($L3_STL$). To implement foldability, a crease is formed at the center of the proposed phased array horizontally with a two-layer structure (L_2 and L_3). Thanks to the crease with a thinner structure, the proposed phased array can be folded without damaging unwanted places.

B. LCP Antennas and Transmission Lines

The designed transmission lines, patch antennas, and their simulation results are described in Fig. 3. Three lines are designed: $L1_MSL$, $L3_STL$, and $L3_MSL$. $L1_MSL$ is used

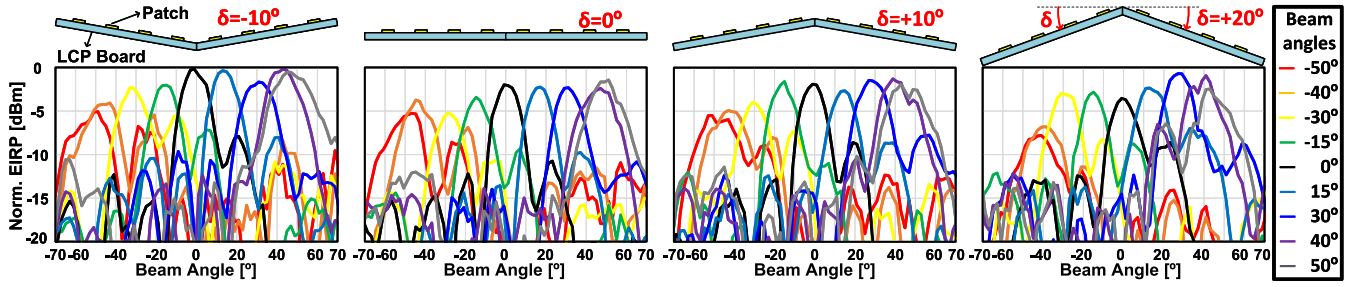


Fig. 6. Measured beam pattern with a linear eight-element array under various board bent-angle states.

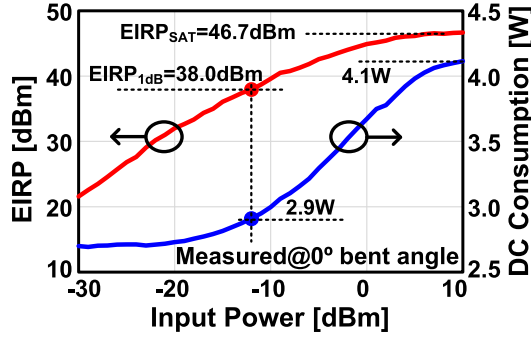


Fig. 7. Measured EIRP with 64-element array along with power sweep.

for antenna driving at the output of the BFICs. L3_STL and L3_MSL are used for the drive of BFIC. While the L3_STL (orange lines in Fig. 2) is used for overall RF signal distribution, L3_MSL (a red line in Fig. 2) runs on the crease which has only L₂ and L₃. The three lines share the L₂ layer as a ground plane.

Due to the two-layer crease structure, the patch antennas next to the crease must have a different design to the patches far from the crease. To compensate for different frequency characteristics, patch sizes, and feeding locations are adjusted as shown in Fig. 3(b) and (c). Two antennas are adopting the proximity feeding method to enhance the bandwidth under the limited number of layers.

C. Calibration of the Deployable Phased Array

In a deployable phased array mounted onto a satellite, the calibration of a mechanically deformed phased array plane geometry is an inevitable process before operating the TX. To calibrate two folded sub-arrays, the beam forming control of two sub-arrays is calculated independently conducted taking bent angle δ into account as described in Fig. 4. Using beam angle and bent angle parameters, the resultant progressive phase difference can be written as

$$\Delta\phi_L = \sin^{-1} \frac{\alpha + \delta}{\beta d_0} \quad (1)$$

$$\Delta\phi_R = \sin^{-1} \frac{\alpha - \delta}{\beta d_0} \quad (2)$$

where d_0 is element spacing which is 5.7 mm and β is the wavenumber at 26.25 GHz.

III. MEASUREMENT

For the evaluation of the proposed deployable active phased array, the 64-element deployable phased array on the LCP board is fabricated as shown in Fig. 5. Fig. 5(a)–(c) illustrates

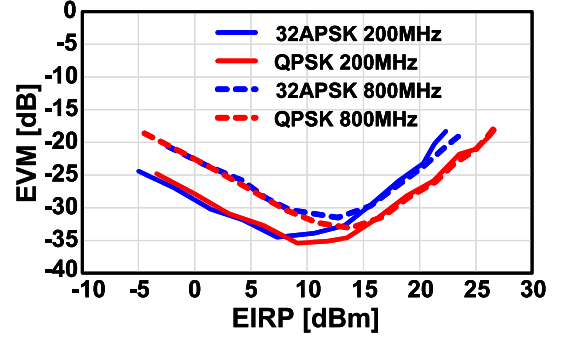


Fig. 8. Measured EVM with linear eight-element array along with the EIRP.

8-element OTA Meas. with 1500MBaud BW				
Modulation	32APSK	256APSK	QPSK	32APSK
Constellation				
EVM [dB]	-28.9	-28.3	-19.1	-21.6
EIRP [dBm]	13.3	12.3	23.2	22.8

Fig. 9. Measured EVM and constellations of different EIRP and modulations.

8-element OTA Meas. With 200MBaud under Bent-Board Condition				
Bent Angle, δ	0°		10°	
Beam Angle, α	0°	30°	0°	30°
Constellation				
EVM [dB]	-34.6	-33.7	-34.5	-31.3
EIRP [dBm]	10.2	10.1	7.3	9.3

Fig. 10. Measured EVM with a 32-APSK modulation signal under different board bent angles.

bent board states. Fig. 5(d) and (e) is the frontside view (ICs) and backside (antennas) view. To drive the 26.25 GHz RF signal, an SMPM connector is utilized. With the flex hetero segment LCP board, the proposed phased-array TX achieved 9.65 g, an extremely lightweight with 64 elements while the TX in [1] is 33.64 g even with 16 elements.

Fig. 6 shows beam patterns with a linear eight-element array under various board bent angles to evaluate the calibration accuracy and beamforming ability.

Fig. 7 illustrates swept electronically isotropically radiated power (EIRP). Maximally, 46.7 dBm of EIRP is achieved with the 64-element array. The proposed deployable active phased array consumes 2.9-W dc power consumption at 38 dBm of EIRP_{1dB}.

The proposed phased-array TX is also tested with DVB-S2Xmodulated signals. The proposed phased-array TX can drive 32APSKmodulation at over the 6 dB back-off power level from the saturatedpower as shown in Fig. 8. Fig. 9 demonstrates that the TX can support a 1.5 Gbaud 256APSKmodulation with -28.3 dB EVM. Under folded board states anddifferent beam angles, the TX achieved less than -31 dB EVM as shown in Fig. 10. Although this work is not using circularpolarization, this work supports the proposed concept, clearly.

IV. CONCLUSION

This work presents a Ka -band 64-element deployable active phased-array TX on an LCP substrate for lightweight and flexibility. To achieve a better flexible crease, this work utilizes combined six-layer and two-layer substrates. Antennas and microstrip lines near the crease are designed and evaluated as well. By controlling each beam of two sub-arrays independently, the proposed deployable active phased-array TX properly works from -10° to $+20^\circ$ bent angle, δ . The proposed deployable phased array can output 46.7 dBm EIRP and support a 1.5 GBaud 32-APSK signal at 6 dB back-off.

REFERENCES

- [1] D. You et al., "A Ka-band 16-element deployable active phased array transmitter for satellite communication," in *IEEE MTT-S Int. Microw. Symp. Dig.*, Jun. 2021, pp. 799–802.
- [2] M. Gal-Katziri, A. Fikes, and A. Hajimiri, "Flexible active antenna arrays," *NPJ Flexible Electron.*, vol. 6, no. 1, p. 85, Oct. 2022, doi: [10.1038/s41528-022-00218-z](https://doi.org/10.1038/s41528-022-00218-z).
- [3] O. S. Mizrahi, A. Fikes, and A. Hajimiri, "Flexible phased array shape reconstruction," in *IEEE MTT-S Int. Microw. Symp. Dig.*, Jun. 2021, pp. 31–33.
- [4] M. Gal-Katziri, A. Fikes, F. Bohn, B. Abiri, M. R. Hashemi, and A. Hajimiri, "Scalable, deployable, flexible phased array sheets," in *IEEE MTT-S Int. Microw. Symp. Dig.*, Aug. 2020, pp. 1085–1088.
- [5] M. R. M. Hashemi et al., "A flexible phased array system with low areal mass density," *Nature Electron.*, vol. 2, no. 5, pp. 195–205, May 2019, doi: [10.1038/s41928-019-0247-9](https://doi.org/10.1038/s41928-019-0247-9).
- [6] X. Wang et al., "A flexible implementation of Ka-band active phased array for satellite communication," in *IEEE MTT-S Int. Microw. Symp. Dig.*, Jun. 2022, pp. 753–756.
- [7] D. You, D. Awaji, A. Shirane, H. Sakamoto, and K. Okada, "A flexible element antenna for Ka-band active phased array SATCOM transceiver," in *Proc. IEEE Asia-Pacific Microw. Conf. (APMC)*, Dec. 2020, pp. 991–993.
- [8] D. You et al., "A Ka-band dual circularly polarized CMOS transmitter with adaptive scan impedance tuner and active XPD calibration technique for satellite terminal," in *Proc. IEEE Radio Freq. Integr. Circuits Symp. (RFIC)*, Jun. 2022, pp. 15–18.